



ISSN: 2230-9926

Available online at <http://www.journalijdr.com>

IJDR

International Journal of Development Research
Vol. 12, Issue, 06, pp. 56448-56452, June, 2022



RESEARCH ARTICLE

OPEN ACCESS

SIMULTANEOUS IMPROVEMENT OF THE ELECTRIC CONDUCTIVE AND MECHANICAL PROPERTIES OF NANOSTRUCTURED ALUMINUM ALLOY

Prazeres E. R.^{1,*}, Loayza C. R. L.¹, Reis V.S.⁴, Melo V. L.⁴; Quaresma J. M. V.⁵; Dos Reis M. A. L.^{1,3}; Silva J. A.S.¹ and Braga E. M.^{1,2}

¹Programa de Pós-Graduação em Engenharia de Recursos Naturais da Amazônia (PRODERNA/ITEC), Federal University of Pará, 66075-110, Belém PA, Brazil; ²Programa de Pós-graduação em Engenharia Mecânica (PPGEM/UFPA), Federal University of Pará, 66075-110, Belém PA, Brazil; ³Faculdade de Ciências Exatas e Tecnologia, Federal University of Pará, 68440-000, Abaetetuba PA, Brazil; ⁴Faculdade de Engenharia Mecânica (FEM/ITEC), Federal University of Pará, 66075-110, Belém PA, Brazil; ⁵Programa de Pós-graduação em Engenharia Industrial (PPGEI/UFPA), Federal University of Pará, 66075-110, Belém PA, Brazil

ARTICLE INFO

Article History:

Received 20th March, 2022
Received in revised form
10th April, 2022
Accepted 27th May, 2022
Published online 22nd June, 2022

Key Words:

Multiwalled Carbon Nanotube,
SS 304 L powder,
H₂O₂, Casting, Nanocomposite.

*Corresponding author:

Prazeres E. R

ABSTRACT

Aluminum nanocomposites demonstrate improvements in mechanical properties, as well as in thermal and electric conductivity. The incorporation of multiwalled carbon nanotubes (MWCNT) in the aluminum matrix, using conventional melting methods, is a long-standing issue. In this paper, Aluminum nanocomposites were fabricated via conventional casting method, using a nanostructured stainless-steel (SS) powder. Carbon nanotubes were treated with hydrogen peroxide, which led to an attachment to the metal matrix particles. In this sense, the SS powder, added as an element alloy, refined the grains, and the CNT led the electric conductivity to a better performance. Given this, the best alloy analyzed presented an approximate 10% increase in all of its characterized properties, therefore presenting a microhardness of 48 HV, a Ultimate Tensile Stress of 183 MPa, and an electrical conductivity of 67% of IACS.

Copyright © 2022, Prazeres et al. This is an open access article distributed under the Creative Commons Attribution License, which permits unrestricted use, distribution, and reproduction in any medium, provided the original work is properly cited.

Citation: Prazeres E. R., Loayza C. R. L., Reis V.S., Melo V. L., Quaresma J. M. V. et al. "Simultaneous Improvement of the Electric Conductive and Mechanical Properties of Nanostructured Aluminum Alloy", *International Journal of Development Research*, 12, (06), 56448-56452.

INTRODUCTION

Pure aluminum had a great level of electric conductivity (~61% IACS), however, its ultimate tensile strength is low (~170 MPa), which encouraged a reinforcement using a steel wire rope – an impractical, expensive, and prolonged process. Elements alloys increment the mechanical properties, but lessen the EC, making it unfeasible. Nanotechnology could provide solutions to this problem, e. g., carbon nanotubes (CNT) have outstanding mechanical and physical properties as low density, tensile strength (~110 GPa), yield module (0.6-5.5 TPa), thermal (6000 W m¹K⁻¹ -SCNT- and 3 000 W m¹K⁻¹ -MWCNT) and electric conductivity (10⁷ to 10⁹ A cm⁻²)^{1,2}; however, its production in a large scale is already restrictive due its high cost of almost 1000 USD/kg.

This price is estimated to drop in the next years, making feasible the use of CNT to substitute the conventional materials³. Currently, they are used as reinforcement of nanocomposites with metal matrices, such as Nickel^{4,5}, Cooper⁶, Iron⁷⁻¹⁰ and, mainly, Aluminum¹¹⁻¹⁴, due to their features of a nanofiber ideal^{15,16}. However, the difficulty in obtaining a uniform distribution and the CNTs agglomerations (clusters) in the matrix caused by Van der Waals forces, in addition to the density disparity between MWCNTs and the aluminum alloy, are long-standing issues in the fabrication of metal composites^{7,8,24}. Aluminum nanocomposites (ANC) are very promising; there are many techniques and research involving the inclusion of CNT in aluminum Metal Matrix (MM), e. g., powder metallurgy^{17,18}, spark plasma sintering¹⁹, hot spark²⁰, mechanical allowing^{21,9}, and stirring casting, i. a., but almost all the processes are very expensive and complex. In addition, they do not avoid agglomeration nor reach structural integrity, and do not have a proper bonding with the MM²².

The stirring casting is quite widespread given the possibility of a greater uniform dispersion of the reinforcement material in the matrix, as well as a lower working temperature, which limits uncontrolled chemical reactions and the appearance of carbides due to high temperatures²³, but the process is prolonged and more expensive than agitation casting^{24,25}. It is necessary to incorporate CNT with conventional casting²⁶, even though high temperatures can destroy the surface integrity of CNTs. This paper presents a methodology that allowed the incorporation of CNTs via conventional casting, increasing both the mechanical properties and electric conductivity.

RESULTS

Figure 1 shows the scheme of the casting and solidification process in the cylindrical metallic mold. For the 0.05C alloy, only carbon nanotubes (0.05 wt.%) were inserted into the liquid metal, and then the mold was poured; it was expected that the carbon nanotube agglomeration would occur, and as the density of CNT is lesser than that of aluminum, they tend to clump on top of the liquid metal^{24,31}. Posteriorly, the CNT was deposited in the mold alongside the first portion of the cast aluminum, and as the solidification occurs quickly, there is not enough time for the CNT to move upwards in the mold, because the first part of the deposited metal, once solidified, holds the nanotubes at the bottom of the produced ingot^{32,33}. The 2SS0.1C alloy (2 wt.% SS-0.1 wt.% CNT) was poured into the mold, as shown in Figure 1. It was noted that part of the mixture disperses in the liquid metal, however, it is expected that the excess mixture will agglomerate at the bottom of the crucible, due to the excess nanostructured powder having a higher density than liquid aluminum³⁴. This behavior resulted in a little amount of the mixture of metallic powder and nanotubes being dispersed in the molten metal, but almost all the elements' alloys were at the bottom of the crucible, reducing the reinforcement effect and deteriorating the properties of the alloy. This decantation could occur due to the limit of solubility of the alloy elements, combined with the low temperature and the melting time³⁵. For the 1SS0.05C alloy (1 wt.% SS-0.05 wt.% CNT), the reinforcement tends to disperse in the matrix when the casting is performed, with a tendency to remain dispersed in the mold, generating the best reinforcement mechanism with an excellent performance³⁴.

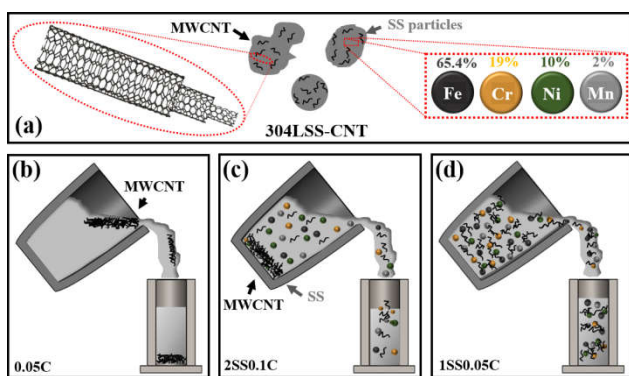


Figure 1. (a) Schematic of the nanostructured powder of 304LSS-5wt.%CNT, with carbon nanotubes and stainless-steel particle. (b) The schematic casting for the aluminum alloy with 0.05wt.% CNT (0.05C), (c) 2 wt.% SS-0.1wt.% CNT (2SS0.1C), and (d) 1 wt.% SS-0.05wt.% CNT (1SS0.05C), as observed for the various nanotube inclusion mechanisms

The alloys obtained were microstructurally characterized using SEM with EDS; the electric conductivity was measured both electrically and mechanically through the microhardness test and the tensile strength test. Figure 2 shows the SEM micrographs and EDS mapping of the Fe to the various alloys, as the (a) shows the typical microstructure of the pure aluminum with low Fe (f) impurity³⁶. The addition of 0.05wt.% CNT (b, g) modified this microstructure, avoiding as egregation of iron to the contour of the dendrites, however, when 1wt.

%SS was incorporated there was a higher precipitation of the alloy's elements into the solute^{24,37}. The addition of the nanostructured powder (304LSS-CNT) with 1wt.%SS-0.05wt.%CNT (d, e) changed the aluminum's microstructures, creating elongated grains with a low segregation of the Fe and of the other elements in the dendrite's limits³⁷. This behavior could be associated with the combination of a decreasing of the grain size by effect to the stainless-steel particles, and a uniform distribution of the carbon nanotubes in the MM, which avoids a bigger movement of the atoms by the effect of the pin with mainly Cr and Ni, whose carbon affinity is great^{10,24}. When the percentage of SS increases to 2 wt.% (e, j), alongside 0.1wt.% CNT, the microstructure was remarkably altered but no segregation was observed, as the temperature of the liquid aluminum was not enough to melt all the SS particles, which produced a deterioration of the properties of this sample³⁷.

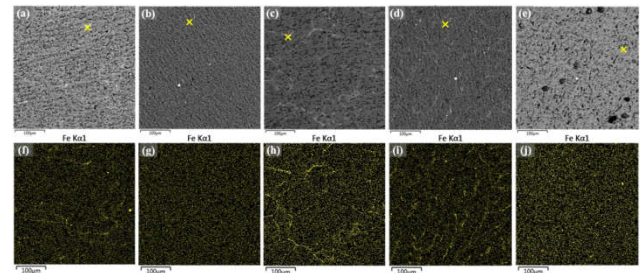


Figure 2. SEM micrographs (top) and EDS mapping (bottom) of the iron (Fe) element alloy for the various samples. (a, f) Pure Al [Al_{Pure}], (b, g) Al-0.05wt.%CNT [0.05C], (c, h) Al-1wt.%SS [1SS], (d, i) Al-1wt.%SS-0.05wt.%CNT [1SS0.05C], and (e, j) Al-2wt.%-0.1wt.%CNT [2SS0.1C]

Raman spectroscopy analyses showed that the Amorphous Carbon Degree (ACD) reduces with the chemical treatment (CT) with hydrogen peroxide, going from 8% for the CNT, as it was received, to 4%¹⁰. The I_D/I_G rate changed from 0.95 to 0.66, resulting in an increment of the crystallinity by effect of the treatment. For the MWCNT, the I_D/I_{Ginner} and I_D/I_{Gouter} rates were 1.1 and 2.6 respectively, varying between 0.99 and 0.98 after selective oxidation, in that order. The high values of the outermost walls' rate (I_D/I_{Gouter}), for the MWCNT, revealed low levels of crystalline, impurities, defective layers, functionalization, and amorphous carbon close to the surface; indeed, the innermost walls had a low rate, indicating a good performance^{8,10,13}. By applying the CT, the rates of both walls were similar, close to one, displaying an improvement of the crystalline. There is a high redshift for the inner (11 cm^{-1}) and outer (26 cm^{-1}) walls, indicated by the G_{inner} and G_{outer} center position. That redshift suggested a tensile strain producing a photon softening (n-doping), as the external walls presented a higher difference, suggesting a great interaction with the MM, which produces a bonding between the carbon nanoparticles and the stainless-steel particles^{8,10,13}. This effect was confirmed by the $\Delta G_{position}$ ($G_{outer}-G_{inner}$) going from 23 cm^{-1} (MWCNT) to 13 cm^{-1} (304LSS-CNT), with the low distance between the peaks indicating a high doping. All this information was supported by the Figure 3, S 01, and S 02. Figure 4 exhibited the XRD patterns for the carbon nanotubes, stainless-steel particles, and the nanostructured powder.

Feature peaks for each material were observed for nanotubes -C(002), C(100), and C(004)- and 304LSS - γ (111), α (110), γ (200), and γ (220), as seen in Figure 4. The nanostructured powder evidenced a reduction in the intensity of the austenitic plane (111), in part due to the superposition with C(100) of the carbon nanotubes, and to the high X-ray absorption capacity of the latter, while the peak C(002) can already be noted in the spectrum^{9,10,38}. All of this proves that the nanostructured powder (304LSS-CNT) was introduced efficiently in the melting aluminum to supply elements alloys such as Fe, Cr, Ni, and Mn of the stainless-steel particles, and nanofibers (MWCNT) to improve both the mechanical properties and electric conductivity^{8,12}. The nanostructured powder is observed in the S 03, as the cluster of CNT is attached to the SS particles. The structural changes by effect

of the chemical treatment (CT) are exhibited in the TEM micrographs of the S 04, as the amorphous carbon disappeared after the CT.

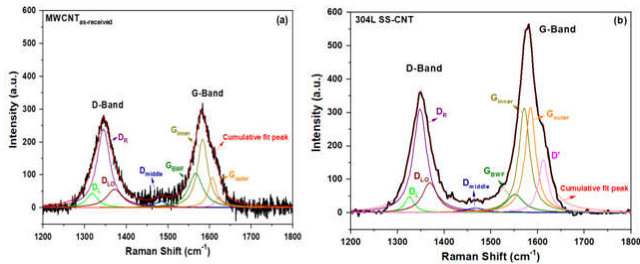


Figure 3. Raman spectroscopy deconvoluted showing the D-band and G-band and their sub-bands D_L , D_R , D_{LO} , $D_{middles}$, D' , G_{BWF} , G_{inner} e G_{outer}

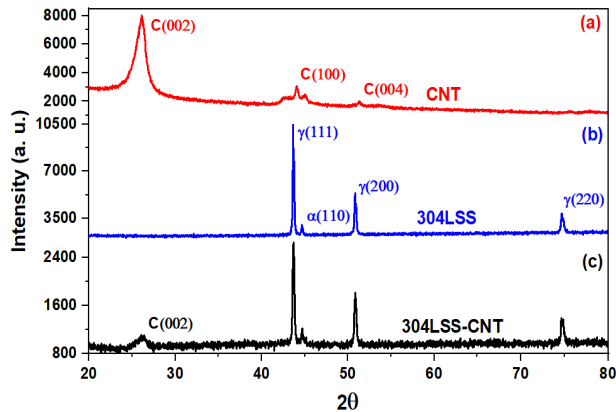


Figure 4. XRD of the (a) as received multiwalled carbon nanotubes, (b) 304L Stainless Steel particles, (c) 304LSS-CNT nanostructured powder

The tensile properties are observed in Figure 5, alongside the dimple rate for each alloy. The curve reveals that the 1SS0.05C had the best results of ultimate tensile strength, toughness, and strain, out of the tested alloys, due to it being combined with the improved mechanical properties resulting from the stainless steel powder and small additions of CNT that, according to the literature, ensure greater homogeneity, consequently reducing the appearance of agglomerates and the accumulation of stress^{10,34}. The 0.05C alloy presented lower results than the other alloys, due to the agglomeration of nanotubes and the low density of the CNT that makes them rise to the surface of the melting metal, as shown in Figure 1b^{24,34,8}. CNT clusters produced an accumulation of punctual stresses, generating areas of failure and reducing the mechanical properties^{34,38}. The dimples ratio, analyzed with the Narayanasamy et al.⁴² method, in which the dimples ratio farther away for one more ductile is the material, showed the superior results of the 1SS0.05C alloy, justifying the reason as to why this material had a better performance of its mechanical properties. Otherwise, the 2SS0.1C alloy showed the most fragile rate through the analyses of the dimples, coinciding with the results of the tensile strength and microstructural analyses^{34,38}.

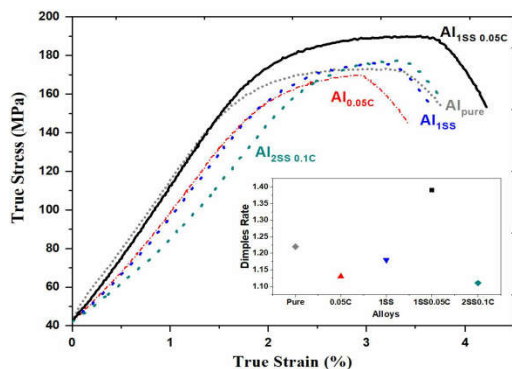


Figure 5. True Strain vs True Stress curve and Dimples ratio for the alloys

Figure 6 shows the fractures after the traction test, together with the dimples' size. Low magnification (80x) presented the characteristic of grabbing the ductile materials, as is the case of aluminum alloys³⁹. The high magnifications (1000x), displaying the dimples, made it possible to obtain an average diameter through a Gaussian curve. The size of the dimples did not vary when comparing the Al_{Pure} to the 0.05C sample, indicating that the incorporation of carbon nanotubes has no influence over the dimples. However, when the stainless-steel particles were added, the size decreased meaningfully in the three samples. For 1wt.% SS samples, the dimples' size, in both samples, was almost the same (~5.6 μm), while with 2 wt% of SS the reduction was more noticeable (~4.7 μm), with a reduction of 23% and 35%, respectively. These results indicated that the SS had a higher effect over the dimples' size than the carbon nanotubes, which was confirmed by the refinement of the grains observed in the macrostructures of the Figure 7.

Figure 7 shows the Ultimate Tensile Strength (UTS), Vickers microhardness (HV0.3), electric conductivity (EC), and macrographs for the samples. Al_{Pure} had the behavior described elsewhere in all of its properties, while the incorporation of 0.05wt.% CNT decreased its performance in UTS, associated with the CNT clusters, acting as stress concentrations and reducing its toughness³⁸. Due to the low density of the CNT, it mainly floated and rose to the surface, remaining only a low quantity in the matrix³⁸. Nevertheless, the EC incremented around 10% to be in accordance with the Al_{Pure}, indicating changes in the properties of the Al matrix. With 1wt.% SS particles powder, the UTS slightly increases, due to the decreasing residual stresses of the alloy elements to the matrix^{12,24}, reducing the deformation and the EC (~5%). The 1SS0.05C sample had a better behavior in all its properties (UTS, strain, toughness, microhardness, and EC), almost 10% in each. It revealed the effect of the chemical treatment nanotubes and their capacity to be attached to the SS powder, effectively connecting the alloy elements of the SS inside the aluminum matrix, maintaining their reinforcement effect^{10,34}. With higher quantities of SS and nanotubes, the reinforcement is compromised, the properties decreasing when compared to the 1SS0.05C sample, but still already above the Al_{Pure}³⁴. High quantities of SS particles powder could not be melted in the aluminum casting, due to low temperature and short time.

The alloy 1SS0.05C showed better results regarding the evaluated properties. In that sense, when compared to the literature, the electrical conductivity was higher than the commercial alloys Al6201 before and after the T81 heat treatment (48.9 %IACS, 50.6 %IACS), in the condition of wire with 3.00 mm in diameter, but the ultimate tensile stress was lower than that obtained in the literature both in the condition before and after the T81 (261.7 MPa and 275.9 MPa)⁴⁰. Al_{Pure} shows coarse equiaxial grains; 0.05C start to refine the central grains, suggesting that the internal heat transfer was higher in the middle of the lingot⁴¹. The addition of 1% of SS particles significantly refines the grains by addition of the alloy elements⁴¹. The addition of 0.05wt.% CNTs refines them even more, due to the high heat transfer from the CNT insertion, while the 2wt.% SS and 0.1wt.% CNT exceed the limit of absorption of the aluminum in this temperature, deriving from a growth of the grains and from lower mechanical, microstructural, and electrical properties^{24,34}.

Conclusion

This work showed a novel process in manufacturing a nanocomposite aluminum alloy with higher mechanical properties and electric conductivity. The best aluminum alloy was the combination of 1 wt.% of stainless-steel particles and 0.05 wt.% of MWCNT, demonstrating 10% of increment in all its properties. The mechanical performance is due to the SS powder and the electric conductivity to the CNT. The bond between the SS powder matrix and the MWCNT, which comes from the chemical treatment applied, is fundamental to incorporate successfully the nanoparticles in the aluminum matrix. The stress-strain curve of the 1SS0.05C alloy had the best results for tensile strength, toughness, and deformation, then the other alloys

tested. With 1% inweight of powdered SS particles and without the CNT, the UTS increases slightly, due to residual stresses arising from the alloying elements to the matrix, reducing strain and electrical conductivity (~5%). The 1SS0.05C sample had a better behavior in all its properties (UTS, deformation, tenacity, microhardness, and EC), an almost 10% increase in each one. This showed the effect of nanotubes with the SS powder, maintaining its reinforcing effect by effectively bonding within the aluminum matrix.

Experimental Procedure

Alloys elements preparation: MWCNT with 95.7% purity and 304L stainless-steel particles sifted until $44 \pm 5 \mu\text{m}$ were the alloy elements. MWCNT was the chemical treatment (CT) with Hydrogen Peroxide, inserted together with the SS 304L powder in an ultrasonic bath (55 kHz, 120 W), with isopropyl alcohol for 10 min; afterwards, the mixture was dried at 130°C to evaporate the H_2O_2 and the isopropyl alcohol^{10,11,14,27,28}.

The crystalline, doping, and amorphous carbon degree of the CNT used a Raman spectroscopy Jovinivon. An equipment Bruker, model 8 Advance with Bragg-Brentano geometry, Lyns Eye detector, Cu tube, $K\alpha_1=1.541$ and Ni filter $K\beta$ performed the X-ray diffraction (XRD) analyses. Micrographs of the nanostructured powder were obtained using a Scanning Electron Microscope (SEM), being displayed in the S 04. TEM micrographs indicated the as-received CNT and the chemical treatment.

Casting procedure: Aluminum was melted to 900°C for four hours. The operational system adopted for the solidification process was the mold in a cylindrical metallic keel consisting of a hollow steel cylinder to obtain a final product of 150 mm length x 25 mm diameter. MWCNT chemical treatment was added to 780°C , measured with a thermocouple, mixed in an inert atmosphere of pure Argon, rate of 0.2 l/s. In 720°C . The mixing process was interrupted, depositing the metal liquid in the mold. Figure 2 shows the solidification modes of the three main alloys, displaying the behavior of each alloy element when only carbon nanotubes, and the nanostructured powder in minor (1SS0.05C) and major amount (2SS0.1C) were added. Five alloys were prepared, Al_{pure} as reference, and four with different content of alloy elements, with 0.05 wt.% CNT (0.05C), 1 wt.% SS (1SS), 1 wt.%SS-0.05 wt.% CNT (1SS0.05C), and 2 wt.%SS-0.1 wt.% CNT (2SS0.1C).

Wire Characterization: A microhmmeter (Megabrás, MPK-2000 model) evaluated the electric conductive of the wires of 3 mm, obtained after a lamination process; over standard ASTM B193-19²⁹. Tensile strength tests were made with a servo pulser Kratos, IKCL1 model, using the standard, ASTM E8/E8M-16a³⁰, with three samples to each alloy. Failure area was analyzed with a SEM. AMitutoyo equipment performed the microhardness Vickers test, with a 3N load, over the standard ASTM E384 – 11. The micrographs and failure analyses utilized a Scanning Electron Microscope (SEM), voltage of 20 kV, with Energy-dispersive X-ray spectroscopy (EDS) for mapping the alloys' elements.

Declaration of Competing Interest: The authors declare that they have no known competing financial interests or personal relationships that could have appeared to influence the work reported in this paper.

Acknowledgement

All authors are grateful to agencies for financial support, for the work teams of the Materials Engineering Research Group (GPEMAT) and the Material Characterization Laboratory (LCAM) of the Federal University of Para (UFPA), where all the experimental tests were performed, and special thanks to the Engineering of Natural Resources of the Amazon Graduate Program (PRODERNA) and National Council for Scientific and Technological Development (CNPq) which provided the C. R. L. scholarships, Number 166397/2017-2 and Number 170412/2017-2. The authors would like to thank the LABNANO/CBPF for technical support during electron

microscopy work. The authors thank PROPEP/UFPA for the financial support regarding the publication costs of this paper.

REFERENCES

- Jagannatham, M. et al. Tensile properties of carbon nanotubes reinforced aluminum matrix composites: A review. *Carbon N. Y.*160, 14–44 (2020).
- Chin, S. Recent progress in the development and properties of novel metal matrix nanocomposites reinforced with carbon nanotubes and graphene nanosheets. *74*, 281–350 (2013).
- Thostenson, E. T., Li, C. & Chou, T. W. Nanocomposites in context. *Compos. Sci. Technol.*65, 491–516 (2005).
- Suarez, S., Lasserre, F. & Mücklich, F. Mechanical properties of MWNT/Ni bulk composites: Influence of the microstructural refinement on the hardness. *Mater. Sci. Eng. A587*, 381–386 (2013).
- Suárez, S., Rosenkranz, A., Gachot, C. & Mücklich, F. Enhanced tribological properties of MWCNT/Ni bulk composites - Influence of processing on friction and wear behaviour. *Carbon N. Y.*66, 164–171 (2014).
- Cha, S. I., Kim, K. T., Arshad, S. N., Mo, C. B. & Hong, S. H. Extraordinary strengthening effect of carbon nanotubes in metal-matrix nanocomposites processed by molecular-level mixing. *Adv. Mater.*17, 1377–1381 (2005).
- Loayza, C. R. et al. Incorporation of AWS 316L wire nanostructured with nickel-carbon nanotube by arc welding. *J. Compos. Mater.* 002199831773588 (2017). doi:10.1177/0021998317735880
- Dos Reis, M. A. L. et al. Raman spectroscopy fingerprint of stainless steel-MWCNTs nanocomposite processed by ball-milling. *AIP Adv.*8, (2018).
- Braga, E. M. et al. A new approach for the reinforcement of SS 304L via arc welding: Using nanostructured flux cored electrode. *Diam. Relat. Mater.*92, 138–145 (2018).
- Borges, D. J. A. et al. Stainless steel weld metal enhanced with carbon nanotubes. *Sci. Rep.*10, 1–13 (2020).
- Simões, S., Viana, F., Reis, M. A. L. & Vieira, M. F. Improved dispersion of carbon nanotubes in aluminum nanocomposites. *Compos. Struct.*108, 992–1000 (2014).
- Rodrigues, F. A. dos S. et al. Electrical and Tensile Properties of Carbon Nanotubes-Reinforced Aluminum Alloy 6101 Wire. *J. Nanosci. Nanotechnol.*17, 4837–4841 (2017).
- Araujo, P. T. et al. Multiwall carbon nanotubes filled with Al4C3: Spectroscopic signatures for electron-phonon coupling due to doping process. *Carbon N. Y.*124, 348–356 (2017).
- Simões, S., Viana, F., Reis, M. A. L. & Vieira, M. F. Microstructural Characterization of Aluminum-Carbon Nanotube Nanocomposites Produced Using Different Dispersion Methods. *Microanal.* 1–8 (2016). doi:10.1017/S143192761600057X
- Ajayan, P. M. & Tour, J. M. Materials Science: Nanotube composites. *Nature* 447, 1066 (2007).
- Lin, D., Saei, M., Suslov, S., Jin, S. & Cheng, G. J. Super-strengthening and stabilizing with carbon nanotube harnessed high density nanotwins in metals by shock loading. *Nat. Sci. Reports* 1–11 (2015). doi:10.1038/srep15405
- Esawi, A. & Morsi, K. Dispersion of carbon nanotubes (CNTs) in aluminum powder. *38*, 646–650 (2007).
- Bakshi, S. R., Lahiri, D. & Agarwal, a. Carbon nanotube reinforced metal matrix composites - a review. *Int. Mater. Rev.*55, 41–64 (2010).
- Bakshi, S. R. et al. Spark plasma sintered tantalum carbide-carbon nanotube composite: Effect of pressure, carbon nanotube length and dispersion technique on microstructure and mechanical properties. *Mater. Sci. Eng. A528*, 2538–2547 (2011).
- Agarwal, A., Bakshi, S. R. & Lahiri, D. *Carbon Nanotubes. Nano Letters*4, (Taylor & Francis, 2011).
- Chen, B. et al. An approach for homogeneous carbon nanotube dispersion in Al matrix composites. *Mater. Des.*72, 1–8 (2015).

22. Zhang, J. *et al.* Carbon science in 2016: Status, challenges and perspectives. *Carbon N. Y.*98, 708–732 (2016).
23. Peng, Y. & Liu, H. Effects of Oxidation by Hydrogen Peroxide on the Structures of Multiwalled Carbon Nanotubes. *Ind. Eng. Chem. Res.*45, 6483–6488 (2006).
24. Hanizam, H., Salleh, M. S., Omar, M. Z. & Sulong, A. B. Optimisation of mechanical stir casting parameters for fabrication of carbon nanotubes-aluminium alloy composite through Taguchi method. *J. Mater. Res. Technol.*8, 2223–2231 (2019).
25. Zeng, X. *et al.* A new technique for dispersion of carbon nanotube in a metal melt. *Mater. Sci. Eng. A527*, 5335–5340 (2010).
26. Marcos Allan Leite dos Reis *et al.* One-Step Synthesis and Characterization of a Nanocomposite Based on Carbon Nanotubes/Aluminum and Its Reinforcement Effect on the Metal Matrix. *J. Mater. Sci. Eng. B5*, 311–319 (2015).
27. Simões, S., Viana, F., Reis, M. A. L. & Vieira, M. F. Effect of dispersion method in the production of Al-CNTs nanocomposites. *Microsc. Microanal.*22, 52–53 (2016).
28. Behler, K., Osswald, S., Ye, H., Dimovski, S. & Gogotsi, Y. Effect of thermal treatment on the structure of multi-walled carbon nanotubes. *J. Nanoparticle Res.*8, 615–625 (2006).
29. Fazio, M., Gutman, E., Hsia, C. & Jones, G. Standard test method for resistivity of electrical conductor materials. *Astm B193-8902*, 1–5 (1990).
30. ASTM E8. ASTM E8/E8M standard test methods for tension testing of metallic materials 1. *Annu. B. ASTM Stand.* 4 1–27 (2010). doi:10.1520/E0008
31. Samuel Ratna Kumar, P. S., Robinson Smart, D. S., & John Alexis, S. (2017). Corrosion behaviour of aluminium metal matrix reinforced with multi-wall carbon nanotube. *Journal of Asian Ceramic Societies*, 5(1), 71-75.
32. Akbari, M. K., Baharvandi, H. R., & Shirvanimoghaddam, K. (2015). Tensile and fracture behavior of nano/micro TiB₂ particle reinforced casting A356 aluminum alloy composites. *Materials & Design (1980-2015)*, 66, 150-161.
33. Ramanathan, A., Krishnan, P. K., & Muraliraja, R. (2019). A review on the production of metal matrix composites through stir casting–Furnace design, properties, challenges, and research opportunities. *Journal of Manufacturing processes*, 42, 213-245.
34. Kuz'Min, M. P., Kuz'mina, M. Y., & Kuz'Mina, A. S. (2019). Production and properties of aluminum-based composites modified with carbon nanotubes. *Materials Today: Proceedings*, 19, 1826-1830.
35. Housaer, F., Beclin, F., Touzin, M., Tingaud, D., Legris, A., & Addad, A. (2015). Interfacial characterization in carbon nanotube reinforced aluminum matrix composites. *Materials Characterization*, 110, 94-101.
36. Rashad, M., Pan, F., Tang, A., & Asif, M. (2014). Effect of graphene nanoplatelets addition on mechanical properties of pure aluminum using a semi-powder method. *Progress in Natural Science: Materials International*, 24(2), 101-108.
37. Hou, J. P., Li, R., Wang, Q., Yu, H. Y., Zhang, Z. J., Chen, Q. Y., ... & Zhang, Z. F. (2019). Origin of abnormal strength-electrical conductivity relation for an Al-Fe alloy wire. *Materialia*, 7, 100403.
38. Liu, Z. Y., Xiao, B. L., Wang, W. G., & Ma, Z. Y. (2014). Tensile strength and electrical conductivity of carbon nanotube reinforced aluminum matrix composites fabricated by powder metallurgy combined with friction stir processing. *Journal of Materials Science & Technology*, 30(7), 649-655.
39. Derpeński, Ł. (2019). Ductile fracture behavior of notched aluminum alloy specimens under complex non-proportional load. *Materials*, 12(10), 1598.
40. Karabay, S. (2006). Modification of AA-6201 alloy for manufacturing of high conductivity and extra high conductivity wires with property of high tensile stress after artificial aging heat treatment for all-aluminium alloy conductors. *Materials & design*, 27(10), 821-832.
41. Zhang, Y., Ma, N., Yi, H., Li, S., & Wang, H. (2006). Effect of Fe on grain refinement of commercial purity aluminum. *Materials & design*, 27(9), 794-798.
42. Narayanasamy, R.; Parthasarathi, N. L.; Ravindran, R.; Sathiya Narayanan, C. Analysis of fracture limit curves and void coalescence in high strength interstitial free steel sheets formed under different stress conditions. Received: 10 May 2007 / Accepted: 11 February 2008 / Published online: 22 March 2008_ Springer Science+Business Media, LLC 2008.
